Observational Study

Medicine®

OPEN

A new 3D printed titanium metal trabecular bone reconstruction system for early osteonecrosis of the femoral head

Ying Zhang, MD, PhD[a], Leilei Zhang, MD[a], Ruibo Sun, MD[a], Yudong Jia, MD[a], Xiantao Chen, MD[a], Youwen Liu, MD[a,*], Hong Oyang, MD[b], Lizhi Feng, MD, PhD[c,*]

Abstract

Presently, biomechanical support therapy for the femoral head has become an important approach in the treatment of early osteonecrosis of the femoral head (ONFH). Previous studies have reported that the titanium metal trabecular bone reconstruction systems (TMTBRS) achieved satisfactory clinical results for the treatment of early femoral head necrosis. Electron beam melting technology (EBMT) is an important branch of 3D printing technology, which enables the construction of an interface that is required for support of bone in-growth. However, the effect of TMTBRS created using EBMT for clinical applications for early ONFH is still unknown. At present, there are no reports on this topic worldwide. The purpose of this study was to assess the safety of a new 3D printed TMTBRS implant and to evaluate its clinical efficacy in early ONFH.

Thirty patients who underwent surgery for ONFH were selected. The stages of ONFH were classified according to the Association Research Circulation Osseus (ARCO) classification. They were followed-up and radiological examination was performed at 6, 12, and 24 months post-surgery to assess TMTBRS stability and bone growth in the bone trabecular holder portion surface. To evaluate hip function, postoperative Harris and Visual Analogue Scale (VAS) scores were used.

The postoperative Harris score increased significantly and VAS score decreased significantly at the 12-month follow-up compared to the 24-month follow-up, wherein the Harris score declined slightly and the VAS score was slightly elevated with the aggravation of ONFH. With the passage of time, postoperative improvement rates were 100% for IIA, 70% for IIB, and 0% for IIC. Hip-preserving rates were 100% for IIA, 100% for IIB, and 50% for IIC.

The effect of TMTBRS treatment for early ONFH in ARCO IIA and ARCO IIB is satisfactory. However, it is not recommended for a relatively large area of necrosis such as in ARCO IIC.

Abbreviations: 3D = three dimensional, ABF = Axon Binary File, ARCO = Association Research Circulation Osseus, BTHP = bone trabecular holder portion, EBMT = electron beam melting technology, ONFH = osteonecrosis of the femoral head, STL = Standard Template Library, THA = total hip arthroplasty, TMTBRS = titanium metal trabecular bone reconstruction system, VAS = visual analogue scale.

Keywords: hip preserving, osteonecrosis of the femoral head, trabecular metal

Editor: Johannes Mayr.

YZ and LZ contributed equally to this work.

Funding: This study was supported by the National Science Foundation of China (81473704) and science and technology project of Henan Province (162102310364). None of the authors of the article had any financial or personal relationships with other people or organizations that could inappropriately influence the work.

Conflict of interest statement: All ICMJE Conflict of Interest Forms for authors are submitted together with the publication and can be viewed on request. Each author certifies that his or her institution approved the human protocol for this investigation, and that all investigations were conducted in conformity with ethical principles of research. Informed consent for participation in the study was obtained. This work was performed at the Hip Center, Luoyang Orthopedic-Traumatological Hospital, Luoyang, China.

The authors have no conflicts of interest to disclose.

[a] *Medical Center of Hip, Luoyang Orthopedic-Traumatological Hospital, Orthopedics Hospital of Henan Province, Luoyang,* [b] *Beijing TianXinFu Medical Appliance Co, Beijing,* [c] *The First Affiliated Hospital of Guangzhou University of Traditional Chinese Medicine, Guangzhou, China.*

[*] *Correspondence: Youwen Liu, Medical Center of Hip, Luoyang Orthopedic-Traumatological Hospital, No. 82, South Qiming Road, 471002 Luoyang, China (e-mail: liuyouwenzhenggu@sina.com); Lizhi Feng, The First Affiliated Hospital of Guangzhou University of Traditional Chinese Medicine, 510006 Guangzhou, China (e-mail: vincent-lucy@163.com).*

Medicine (2018) 97:26(e11088)

Received: 16 July 2017 / Accepted: 22 May 2018

http://dx.doi.org/10.1097/MD.0000000000011088

1. Introduction

Presently, conservative treatments of osteonecrosis of the femoral head (ONFH) include medications and surgeries.[1,2] Early hip-preserving treatments are particularly important for young patients.[3,4]

Support therapy of the femoral head has become an important tool in the treatment of early ONFH. 3D printing technologies allow the construction of the object layer by layer using powdered metal or plastic bondable materials.[5] Electron beam melting technology (EBMT) is an important branch of 3D printing technology, which enables the construction of an interface that is required for support of bone in-growth.[6]

The titanium metal trabecular bone reconstruction system (TMTBRS) consists of a bone trabecular holder portion (BTHP) and a connecting rod (Figs. 1–4). The solid and porous layers of the TMTBRS created using the EBMT technology are formed at the same time.[7] BTHP is formed between the grid and it criss-crosses throughout the bone pores. As these pores are interconnected, the bone tissue can easily grow in it, as the body recognizes human bones and BTHP as one structure.[8] However, the effect of TMTBRS created using EBMT in clinical applications for early ONFH is still unknown. At present, there are no reports on this topic worldwide.

This prospective study was designed to investigate the effects of 3D printed TMTBRS and decompression surgery in early ONFH, to analyze the safety of using TMTBRS, and to assess its clinical efficacy.

2. Materials and Methods

2.1. Process and characteristics of 3D-printed TMTBRS

The EBMT manufacturing equipment rapid prototyping device was purchased from Arcam AB (Mölndal, Sweden), a Swedish company (Model S-12, Fig. 1). The technical parameters used for trabecular support by 3D printing manufacturing applications in this study were as follows: working space size: 250 mm × 250 mm × 200 mm; maximal size of product: 200 mm × 200 mm × 180 mm; maximal power of the electron beam of 3000 W; electron beam diameter of 180 μm; melting speed of 55 to 80 cm^3/h (for Ti6Al4V material); and degree of vacuum work area $<1 \times 10^{-4}$ mbar.

The preparation process of the matrix was as follows: UG software (Siemens PLM Software, Germany) was used to design the 3D solid model of the TMTBRS in a professional computer; the 3D entity model was imported through the dedicated STL (Standard Template Library) editing software (Magics Edit, Materialise, Belgium), repaired, arrayed, and scaled; using Arcam EBMT Build Assembler software (Arcam, Sweden), the imported file was processed, wherein the layer thickness was selected and ABF (Axon Binary File) format scanning procedures for control of melt molding equipment were generated; the ABF file was imported into the EBMT electron beam melting rapid prototyping equipment; the powder hopper was filled with titanium alloy powder, and the diameter of the powder particle was 45 to 105 μm; to start the plate, the door was closed, vacuum pump was opened, and vacuum processing module was set at $<1 \times 10^{-4}$ mbar; the electron beam preheating starting disk was heated to 730°C; the use of powder was uniform on the work table, and the thickness of the flat metal powder layer was 0.07 mm; the electron gun was controlled by the computer and, according to the scan data, the electron beam was focused onto the titanium alloy powder layer on the surface of the working platform. The process of electron beam in each layer was divided into the following stages: heating and melting. The metal powder in the average current electron beam was under the action of melt solidification. The electron beam in the process of molten pool temperature can reach >1800°C; the working table was controlled by the computer to drop a layer of height, and the titanium alloy powder was again evenly spread on the table. Then, the electron beam melting process was repeated, and the current and previous

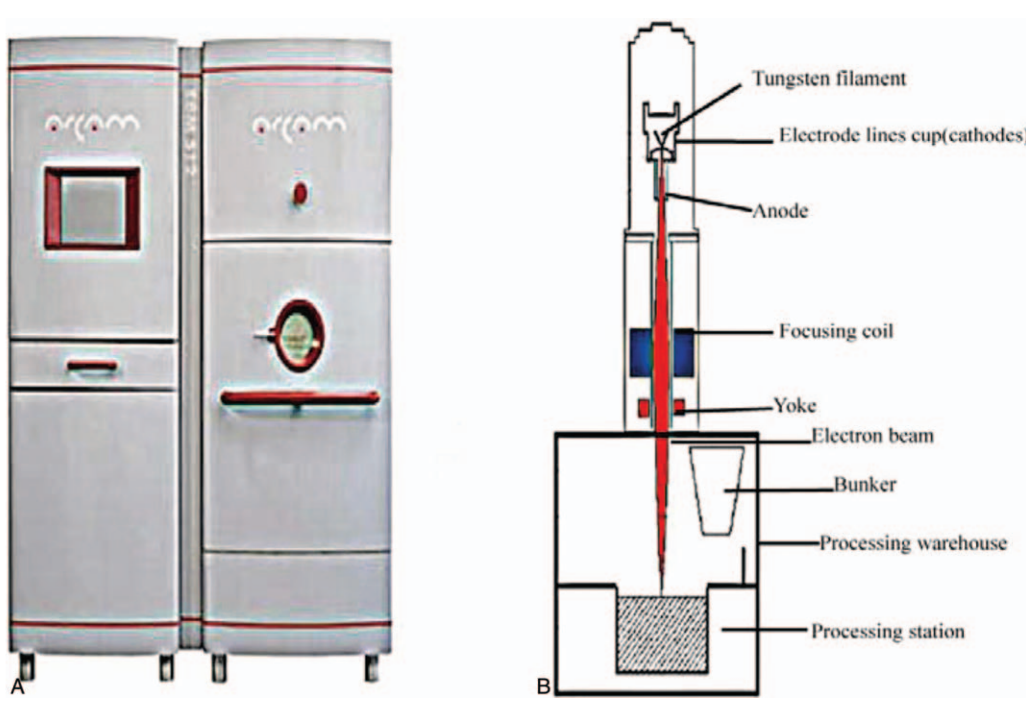

Figure 1. Electron beam melting technology rapid prototyping equipment (A) and electron beam processing diagram (B).

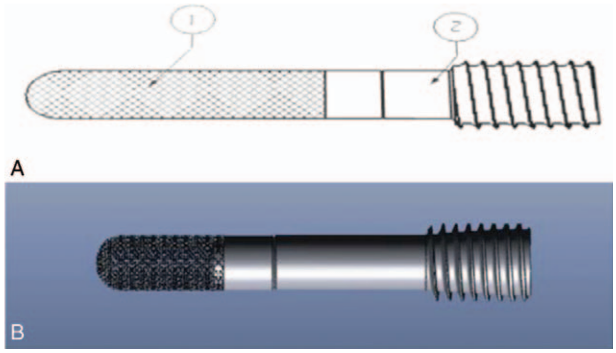

Figure 2. Trabecular metal structure of titanium metal trabecular bone reconstruction system (A, B). A1 is the bone trabecular holder portion and A2 is the connecting rod.

layers with the melted area were melted as a whole. It was not stacked until the product processing was completed; after the completion, helium was processed to 400 Pa to rapidly cool down the product; following the cool down, the product was placed together with the sintering of the powder around the tray on the starter plate. The parts were transferred to the powder recovery system. Clean compressed air mixed with Ti6Al4 V powder was used to clean the products. Subsequent processing was not over until the final product was completed (a schematic representation of the process is presented in Fig. 2).

2.2. Patients

All patients were selected from the medical hip center of our hospital from June 2014 to November 2015. All patients underwent preoperative examination, including physical, laboratory, and imaging examinations. The stages of ONFH Association Research Circulation Osseus (ARCO) stage II were classified according to the ARCO classification. Patients with ONFH were identified through the individual diagnosis of three physicians currently. The study has been approved by the ethics committee of the Luoyang Orthopedic Traumatological Hospital (CS2014–025). The inclusion criteria were as follows: patients of both sexes aged from 18 to 55; ONFH was classified into ARCOII stages[9]; absence of mental illness, systemic disease, history of alcoholism or drug abuse, and femoral head distortion; capable of communicating with the researchers and complied with the requirements of the entire study; and voluntarily entered the study and signed the informed consent. The exclusion criteria are as follows: patients suffering from severe cardiocerebrovascular disease, ankylosing spondylitis, or atrophic arthritis.

2.3. Surgical methods

We operated under G-arm fluoroscopy. An incision (about 3 cm) was made at the lateral hip region and we exposed the lateral femoral cortex and 2-center tunnel line, which can be found in the necrotic lesion area center and a little above the lesser trochanter of the femur. The cortical bone was determined based on the thick-to-thin transition with the small rotor counterpart.

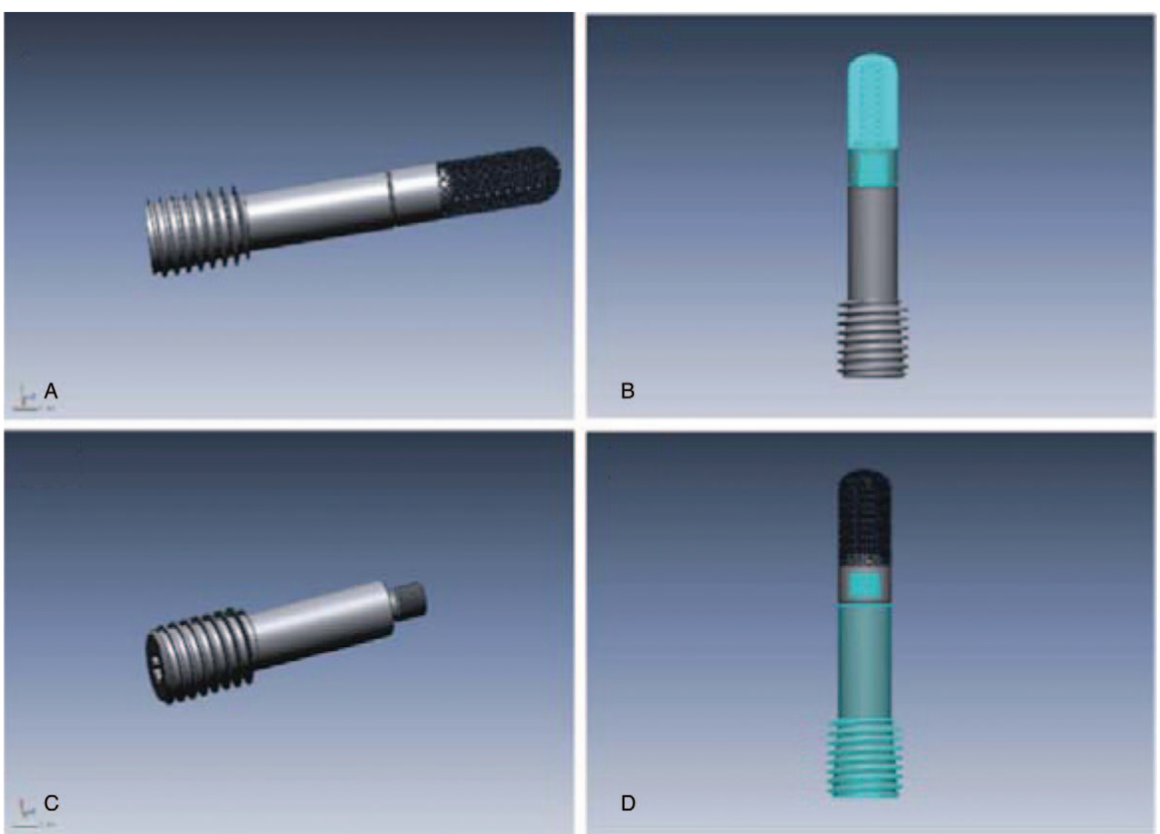

Figure 3. The split design of the titanium metal trabecular bone reconstruction system. Its chemical composition is in line with the provisions of YY0117.2 (A) Titanium metal trabecular bone reconstruction system split design of the connecting rod with its chemical composition in line with GB/T 13810 in the grades specified by TC4ELI. (B) Titanium metal trabecular bone reconstruction system split design of the bone trabecular holder portion, the intermediate hollow design. Bone induction material with treatment can be implanted in the middle (C).

Rotation (10–15 degree) within the joint itself was made to remove the femoral neck anteversion. The lateral femoral coronal plane of the intermediate of the femroral neck was determined. The tip of the needle of the guide pin was located about 5 mm inside the femoral head surface.

First, we removed the bone of the greater trochanter with a circular bone removal apparatus for spare bone. Then we gradually reamed the hole. The same diameter was selected for the final trabecular bone substitute. The maximum depth of the hole was about 5 mm below the femoral head surface. To determine the required length of TMTBRS, the guide needle was removed and the insertion depth was used to measure the length. The appropriate size and length of the extension rods were selected, and the taped wire was used to connect the T-handle. We entered though the lateral femoral cortical bone and wire-taped in a clockwise direction. All threaded portions corresponding to the length of the taped wire were located entirely within the cortical bone. We used a spatula to remove the necrotic tissue after performing a biopsy. Autologous cancellous bone harvested from the greater trochanter or bone allograft harvested in the area of the femoral head necrosis in the femoral head and impaction grafting. Bone induction material was implanted and placed in the hole in the middle of the BTHP, and then the most appropriate metal TMTBRS was implanted.

All patients were instructed to avoid weight-bearing activities completely for 2 weeks. Partial weight bearing was allowed at 4 to 6 weeks post-surgery and full weight-bearing was allowed 6 weeks post-surgery. Twenty-four hours after surgery, injections of low-molecular-weight heparin calcium (0.4 mL) were administered daily for 14 continuous days. An intermittent pneumatic compression device was used twice daily since the first day post-surgery for 30 minutes each time for 14 continuous days.

2.4. Follow-up and treatment evaluation

Patients were followed up at 6, 12, and 24 months post-surgery. The Harris score was used before and after surgery and during the follow-up to evaluate the efficacy of the intervention based on pain level, joint function, and mobility, with a total score of 100 points. A score ≥90 was considered excellent, ≥80 was good, ≥70 was normal, and <70 was poor. The Visual Analog Scale (VAS) is a measurement instrument that measures patients' pain, and is scored as follows: 0, no pain; 1 to 3, a slight pain and can be endured; 4 to 6, pain that affects sleep, but can still be endured; and 7 to 10, gradually strong pain that affects appetite and sleep. Radiographic self-assessment was used to estimate the position of TMTBRS and bone growth. Reconstructed radiolucent lines around the TMTBRS and their shifts were also monitored.

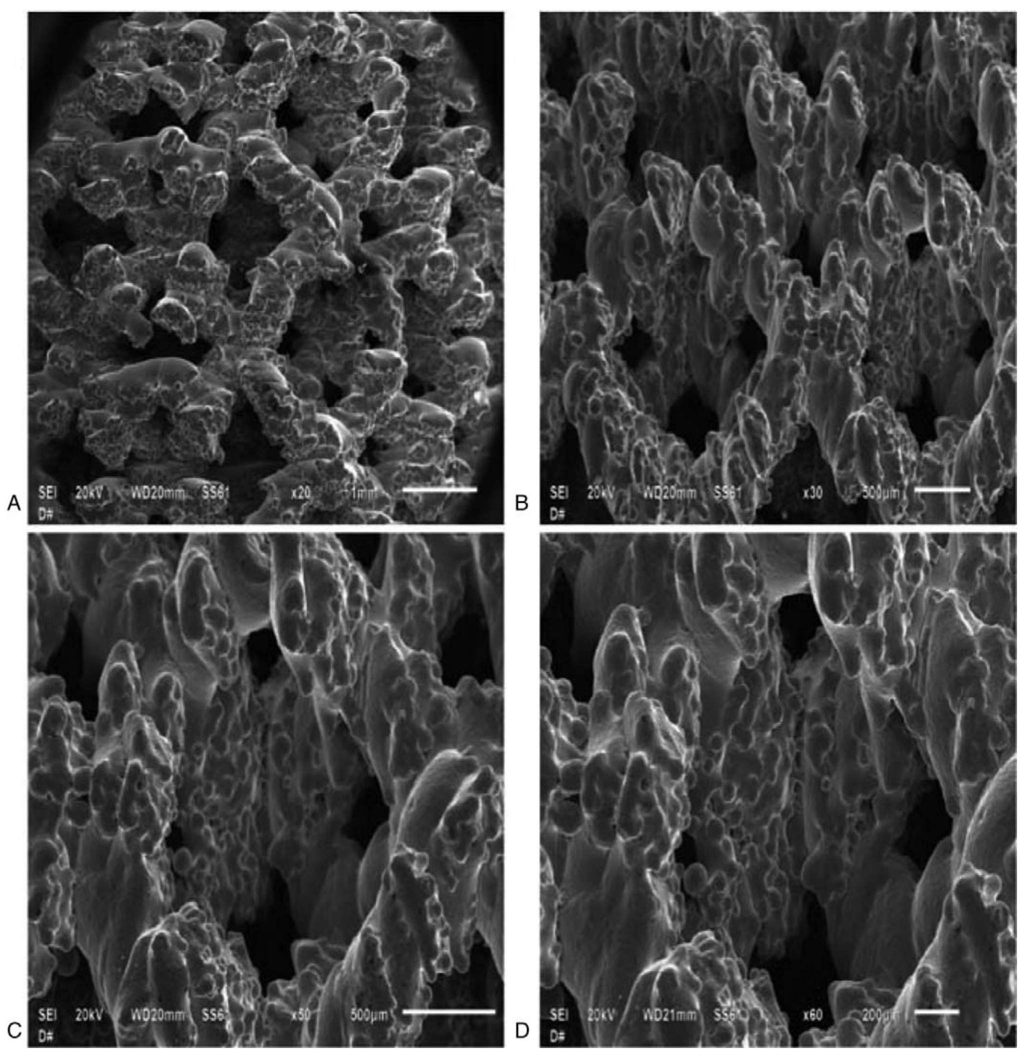

Figure 4. Trabecular metal-holder SEM Fig, 20× (A), 30× (B), 50× (C), 60× (D).

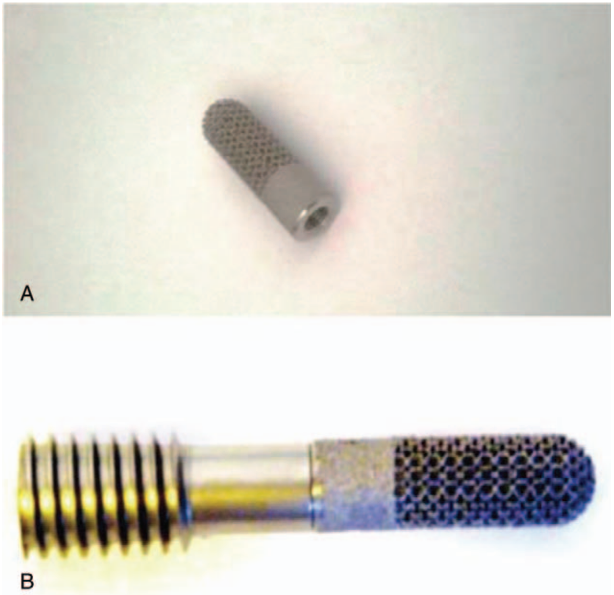

Figure 5. Physical appearance of bone trabecular holder portion (A) and titanium metal trabecular bone reconstruction system (B).

Patients who are candidates for standard total hip arthroplasty (THA) surgery (Grade IV) were considered to have failed the hip preservation treatments.

Anteroposterior and frog-like (or axial) TMTBRS bone growth and stress shielding were observed with the following characteristics: TMTBRS shift or appearance of 3 partitions with at least a 1-mm radiolucent line was considered unstable; and if 1 partition appeared, the strength of the regional trabecular bone was considered to recreate stress shielding arrangement. A line along the central region of the TMTBRS in the femoral head and a vertical line at the neck junction were drawn, which divided the TMTBRS into 4 zones (Figs. 5 and 6).

According to previously proposed methods of the authors, the imaging evaluation methods of the proposed 4 levels mainly depend on the degree of collapse and necrosis (Fig. 7).

2.5. Data analysis

The STATA software, version 12.0 (Stata Corp, College Station, TX) was used for data processing. Quantitative data were expressed as mean ± standard deviation. A comparison of the data between the preoperative and follow-up periods after treatment was performed using Dunnett test. Statistical difference was considered significant at $P < .05$.

3. Results

Thirty patients were included in the study (Fig. 8). All patients were followed-up for 24 months, and they successfully completed the study.

3.1. Harris score

The results showed that changes in the Harris score were statistically significant ($P = .003$). Harris scores following no treatment and at 6, 12, and 24 months post-surgery were statistically significant ($P = .017$), individually (Fig. 9).

3.2. VAS score

The results showed that changes in the VAS score were statistically significant ($P = .006$). VAS scores following no treatment and at 6, 12, and 24 months post-surgery were statistically significant ($P = .012$), individually (Fig. 9).

3.3. Changes in x-ray images staging

The results showed that at the last follow-up period, ONFH had progressed in varying degrees. This shows that support surgery cannot completely stop the progress of ONFH, but may be effective in delaying its progression (Fig. 10).

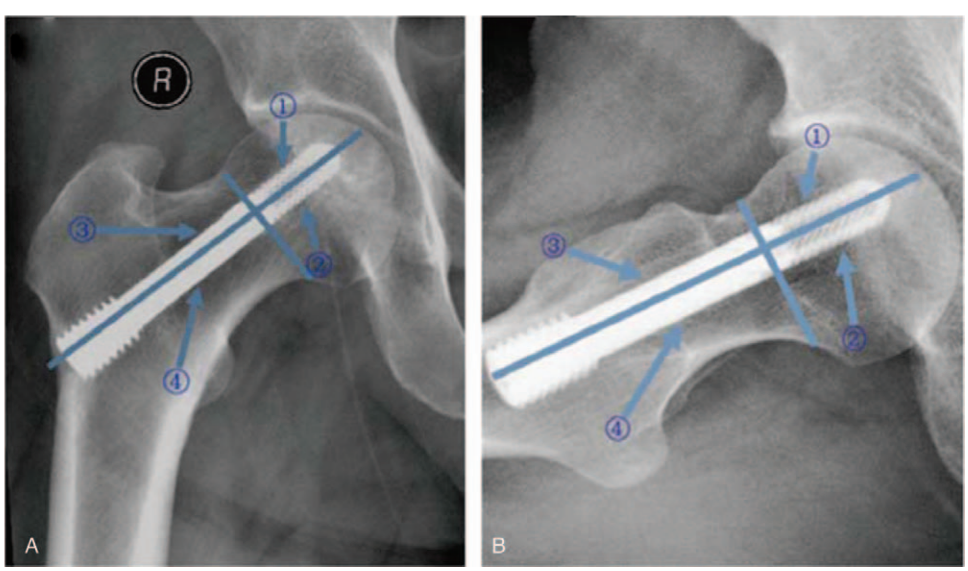

Figure 6. Anteroposterior (A) and lateral (B) views of the implanted bone in growth and evaluate stress shielding partition schematic.

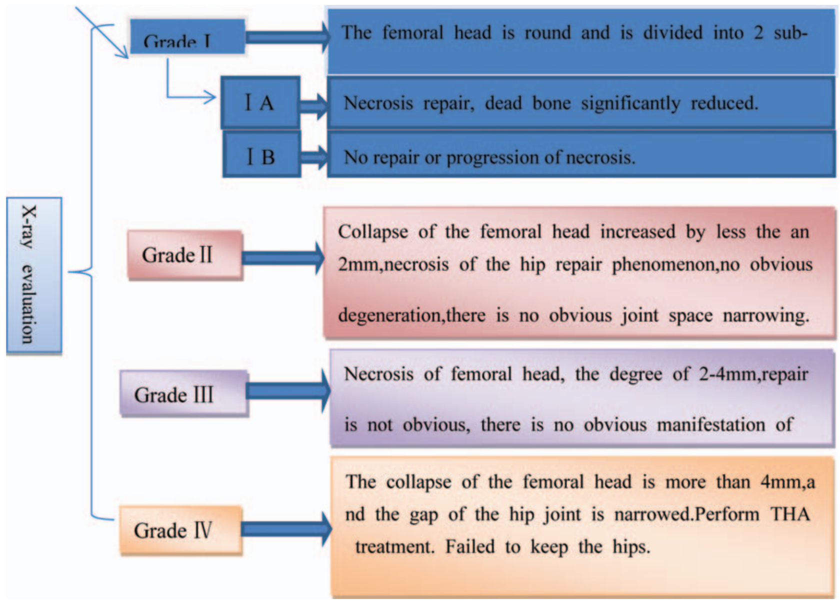

Figure 7. Imaging evaluation method: according to the method previously proposed by the authors, evaluation was improved, primarily on the basis of necrosis and collapse of self-made 4 grades. THA = total hip arthroplasty.

3.4. Changes of x-rays images

Assessment of bone growth and stress shielding showed that, after 1 week, 8 partitions (120 partitions in total) and 8 partitions (120 partitions in total) appeared as radiolucent lines on the anteroposterior and lateral x-ray films, respectively. All translucent partition lines disappeared at 6 months, and no new radiolucent lines appeared on the x-ray film. No bone enhancement occurred in the first region of the femoral head during the follow-up period. Stress shielding and trabecular bone enhancement did not occur in any of the regions.

3.5. Hip-preserving ratio and improvement rates

The results showed that postoperative improvement rate was 100% for IIA, 70% for IIB, and 0% for IIC. Judging from the 2 sets of statistics, the improvement rate and hip protection ability of IIA and IIB were clearly superior to IIC, whereas IIC's hip protection was only half the rate of those of IIA and IIB. Patients showed no signs of infection or rejection (Fig. 11).

4. Discussion

ONFH is an unsolved problem in bone science, especially when it occurs in young adults (30–50 years' old). If not treated, it

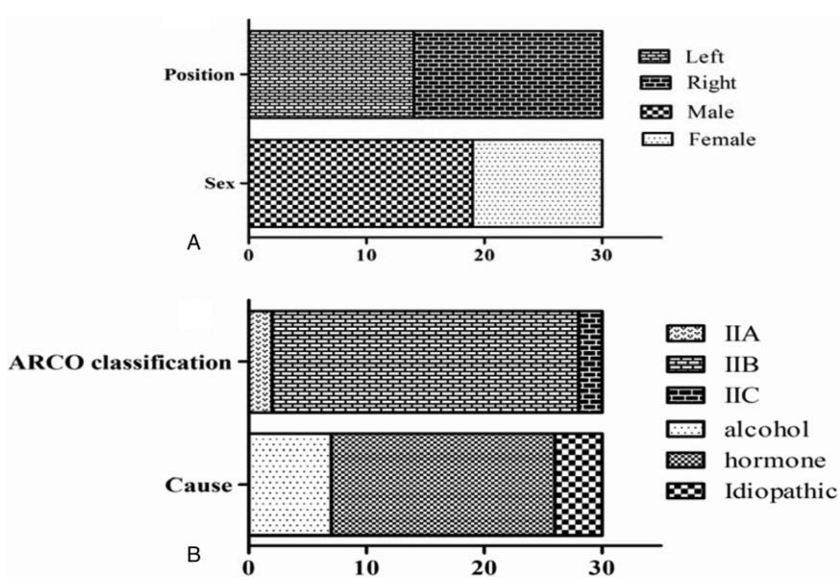

Figure 8. Characteristics of the patient's condition. The patients included 19 males and 11 females (A) and 14 left hips and 16 right hips (A), with ages ranging from 22 to 54 years (average 41.72 ± 3.56 years). Patients' ARCO staging indicated 2 hips of stage II A, 26 hips of stage II B and 2 hips of stage II C (B). ARCO = Association Research Circulation Osseus.

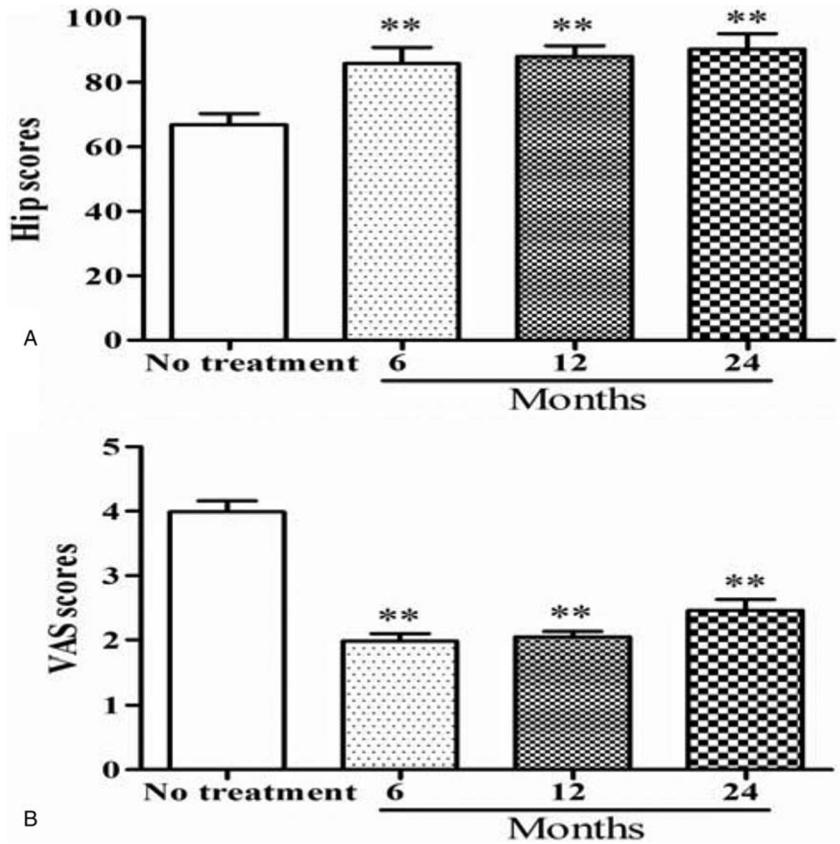

Figure 9. Harris and Visual Analogue Scale (VAS) scores. Hip joint function score in patients before and after treatment (A). VAS score in 2 groups of patients before and after treatment (B). Data are shown as means ± standard deviation at the 24th month. $^{**}P < .01$ vs. no treatment.

eventually leads to collapse of the femoral head, osteoarthritis, and disability, which require THA.[10] However, THA prosthesis longevity and other factors are poor.[11] THA is not recommended for early ONFH, especially in young patients. Therefore, hip preservation becomes an important therapeutic principle.[12,13] The features of hip-preserving surgery include: reducing joint capsule pressure; removal of necrotic tissue; the use of tantalum rod or autogenous bone supporting the femoral head to prevent its collapse and deformation; increasing blood supply to the femoral head; bone repair mechanism preventing regional necrosis and further collapse of the femoral head; and prolonging

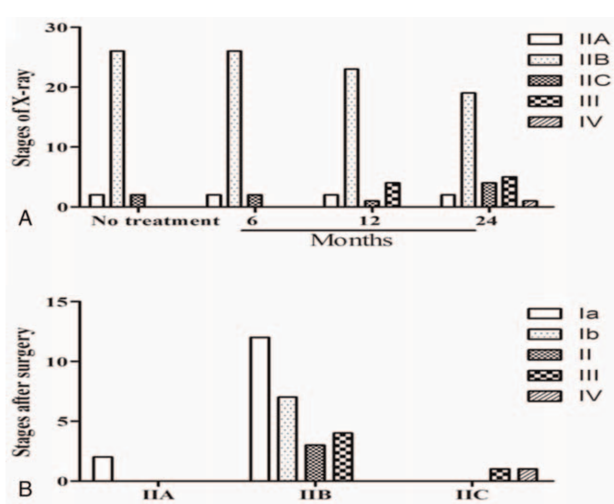

Figure 10. Preoperative and postoperative x-ray images staging and follow-up for 24 months. Radiographic assessment for 24 months showed that the level I patients are in better condition, and have not reached a final grade of IV.

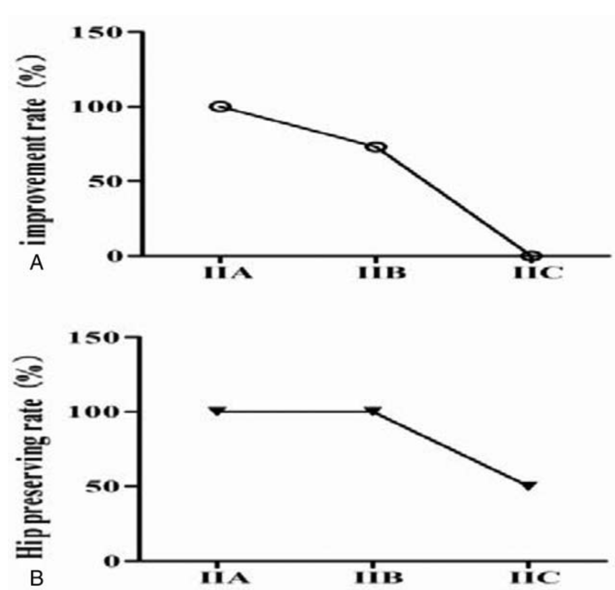

Figure 11. The rate of improvement and hip preservation. The results showed that postoperative improvement rate was 100% of IIA, 70% of IIB, and 0% of IIC (A). Judging from the 2 sets of statistics, the improvement rate and protection of the hips of IIA and IIB patients were superior to IIC.

autologous hip use time.[14] Treatment of ONFH depends mainly on its stage, as well as the surgeon's clinical choices.[15] ONFH treatment focuses on effectively improving symptoms and delaying the need for a hip replacement surgery. Traditional hip-preserving surgery methods included pressure reduction, rotational osteotomy, free bone grafts, and vascularized bone transplantation.[16–18]

3D printing technology uses powdered metal or plastic bondable material to construct the desired object layer by layer. Without using machinery or molds, various parts can be created directly based on computer graphics data. This greatly shortens the product development cycle, improves productivity, and reduces production costs. Worldwide, 3D printing has received great attention in the industry, and therefore, 3D printing technology is known as one of the industrial revolutions, which may subvert the traditional manufacturing model.[19] EBMT technology is an important branch of 3D printing. The use of EBMT technology can achieve the desired bone growth interface, trabecular support for the physical layer, and metal surface of the porous layer fabricated for bone tissue regeneration. The porous trabecular bone holder portion is formed between the grid and it criss-crosses throughout the pores. As these pores are interconnected, the bone tissue and trabecular bone holder combine, making human bones and trabecular support seamless. Studies have shown that titanium porous surface EBMT, prepared based on superior biological properties, can promote cell attachment, growth, and stem cell osteogenic differentiation.[20–22] Biological materials can increase the metal-binding capacity of cells,, thus greatly increasing bone prosthesis metal-binding capacity, which results in better mechanical properties.[23]

The trabecular metal avascular necrosis reconstruction rod has been used for early ONFH. The porous tantalum rod has unique physical and mechanical characteristics. It has high volume porosity (>80%) and allows complete communication among the pores (Fig. 4), which results in reliable and rapid bone growth.[24] Its elastic modulus and bone closure can reduce stress shielding. It is a structured material, and the finished implant has sufficient strength to withstand the physiological load.[25] It was also found that the elastic modulus of the porous tantalum rod and fibula in the femoral head underwent the same stress and strain modes. The most porous tantalum rod withstands pressure rather than bending and tension. The best porous tantalum rod implant was positioned on the outer side of the femur, so that it contacts and supports the subchondral bone plate, playing a supportive role. The joint use of porous tantalum rod implant and core decompression treatment of femoral head necrosis can provide structural support for the subchondral bone, delay femoral head collapse, and delay the need for THA.[26–28] However, once the femoral head collapses and needs to be replaced, it is difficult to remove the tantalum rod.

The partially microporous compressive strength is >20 MPa. Microporous pore portion of 50% to 80% allows enough space for bone growth. The size of the microporous portion is approximately 300 to 700 μm (Figs. 2–4).

This present study has several weaknesses. First, this was an observational study and had all the limitations of observational studies, group no comparison between the control group and the control group. Second, there was no control group in this study. Third, because of the small number of treated patients, the power of the statistics was low and the interpretation of data was relatively limited. Thus, further studies with expansion of the sample size and prospective randomized controlled trials are needed to verify our conclusion.

We conclude that the 3D-printed TMTBRS implant is effective and reliable. In addition, it requires minimally invasive surgery, it is easy to grasp, and its split structure makes it easy to remove and to perform THA if needed. TMTBRS is an effective treatment for early ONFH. In cases of ONFH in early ARCO IIB, this treatment is satisfactory, but in cases with a large necrotic area such as in ARCO IIC, it is not recommended. For BTHP, the bone-inducing material can easily be implanted into the hollow structure to improve the curative effect.

Author contributions

Data curation: Ruibo Sun, Xiantao Chen.
Formal analysis: Xiantao Chen.
Investigation: Hong Oyang.
Methodology: Lizhi Feng, Youwen Liu.
Project administration: Youwen Liu.
Software: Lizhi Feng.
Supervision: Yudong Jia, Leilei Zhang.
Writing – original draft: Ying Zhang, Leilei Zhang.

References

[1] Gatin L, Rogier DMA, Mary P, et al. Osteonecrosis of the femoral head: a proposed new treatment in homozygous sickle cell disease. Hemoglobin 2016;40:01–9.
[2] Zhang Y, Liu Y, Zhou G, et al. Fibular allograft for osteonecrosis prevention in the management of femoral neck fractures: clinical outcome and biomechanical evaluation. J Biomater Tiss Eng 2015; 5:937–41.
[3] Bravo D, Wagner ER, Larson DR, et al. No Increased risk of knee arthroplasty failure in patients with positive skin patch testing for metal hypersensitivity: a matched cohort study. J Arthroplasty 2016;31: 1717–21.
[4] Zhou G, Zhang Y, Zeng L, et al. Should thorough debridement be used in fibular allograft with impaction bone grafting to treat femoral head necrosis: a biomechanical evaluation. BMC Musculoskelet Disord 2016;16:140–8.
[5] Shim JH, Yoon MC, Jeong CM, et al. Efficacy of rhBMP-2 loaded PCL/PLGA/beta-TCP guided bone regeneration membrane fabricated by 3D printing technology for reconstruction of calvaria defects in rabbit. Biomed Mater 2014;9:065006.
[6] Lv J, Xiu P, Tan J, et al. Enhanced angiogenesis and osteogenesis in critical bone defects by the controlled release of BMP-2 and VEGF: implantation of electron beam melting-fabricated porous Ti6Al4V scaffolds incorporating growth factor-doped fibrin glue. Biomed Mater 2015;10:035013.
[7] Krych AJ, Howard JL, Trousdale RT, et al. Total hip arthroplasty with shortening subtrochanteric osteotomy in Crowe type-IV developmental dysplasia. J Bone Joint Surg Am 2009;91:2213–21.
[8] Nunez FA, Arguelles AA, Lozano LL, et al. [Use of trabecular metal in total knee arthroplasty in severely and morbidly obese patients (BMI> 35 kg/m2)]. Acta Ortop Mex 2013;27:97–102.
[9] Song H, Tao L, Wang F, et al. Effect of bone mesenchymal stem cells transplantation on the micro-environment of early osteonecrosis of the femoral head. Int J Clin Exp Pathol 2015;8:14528–34.
[10] Clement RG, Ray AG, MacDonald DJ, et al. Trabecular metal use in paprosky type 2 and 3 acetabular defects: 5-year follow-up. J Arthroplasty 2016;31:863–7.
[11] Zhao DW, Yu M, Hu K, et al. Prevalence of nontraumatic osteonecrosis of the femoral head and its associated risk factors in the chinese population: results from a nationally representative survey. Chin Med J (Engl) 2015;128:2843–50.
[12] Yin W, Xu Z, Sheng J, et al. Logistic regression analysis of risk factors for femoral head osteonecrosis after healed intertrochanteric fractures. Hip Int 2016;26:215–9.
[13] Kubo T, Ueshima K, Saito M, et al. Clinical and basic research on steroid-induced osteonecrosis of the femoral head in Japan. J Orthop Sci 2016;21:407–13.
[14] Liu D, Li X, Li J, et al. Knee loading protects against osteonecrosis of the femoral head by enhancing vessel remodeling and bone healing. Bone 2015;81:620–31.

[15] Genereux P, Stone GW, O'Gara PT, et al. Natural history, diagnostic approaches, and therapeutic strategies for patients with asymptomatic severe aortic stenosis. J Am Coll Cardiol 2016;67:2263–88.

[16] Sun Y, Feng Y, Zhang C. The effect of bone marrow mononuclear cells on vascularization and bone regeneration in steroid-induced osteonecrosis of the femoral head. Joint Bone Spine 2009;76:685–90.

[17] Yen CY, Tu YK, Ma CH, et al. Osteonecrosis of the femoral head: comparison of clinical results for vascularized iliac and fibula bone grafting[J]. J Reconstr Microsurg 2006;22:21–4.

[18] Lieberman JR, Engstrom SM, Meneghini RM, et al. Which factors influence preservation of the osteonecrotic femoral head? Clin Orthop Relat Res 2012;470:525–34.

[19] Spetzger U, Frasca M, Konig SA. Surgical planning, manufacturing and implantation of an individualized cervical fusion titanium cage using patient-specific data. Eur Spine J 2016;25:2239–46.

[20] Van de Kelft E, Van Goethem J. Trabecular metal spacers as standalone or with pedicle screw augmentation, in posterior lumbar interbody fusion: a prospective, randomized controlled trial. Eur Spine J 2015; 24:2597–606.

[21] Grappiolo G, Loppini M, Longo UG, et al. Trabecular metal augments for the management of paprosky type III defects without pelvic discontinuity. J Arthroplasty 2015;30:1024–9.

[22] Sandow M, Schutz C. Total shoulder arthroplasty using trabecular metal augments to address glenoid retroversion: the preliminary result of 10 patients with minimum 2-year follow-up. J Shoulder Elbow Surg 2016; 25:598–607.

[23] Huang DY, Zhang L, Zhou YX, et al. Total Hip arthroplasty using modular trabecular metal acetabular components for failed treatment of acetabular fractures: a mid-term follow-up study. Chin Med J (Engl) 2016;129:903–8.

[24] Bobyn JD, Stackpool GJ, Hacking SA, et al. Characteristics of bone ingrowth and interface mechanics of a new porous tantalum biomaterial. J Bone Joint Surg Br 1999;81:907–14.

[25] Chevalley T, Bonjour JP, van Rietbergen B, et al. Tracking of environmental determinants of bone structure and strength development in healthy boys: an eight-year follow up study on the positive interaction between physical activity and protein intake from prepuberty to mid-late adolescence. J Bone Miner Res 2014;29:2182–92.

[26] Hirota M, Hayakawa T, Ohkubo C, et al. Bone responses to zirconia implants with a thin carbonate-containing hydroxyapatite coating using a molecular precursor method. J Biomed Mater Res B Appl Biomater 2014;102:1277–88.

[27] Ahmad AQ, Schwarzkopf R. Clinical evaluation and surgical options in acetabular reconstruction: A literature review. J Orthop 2015;12: S238–243.

[28] Papi P, Jamshir S, Brauner E, et al. Clinical evaluation with 18 months follow-up of new PTTM enhan ced dental implants in maxillo-facial post-oncological patients. Ann Stomatol (Roma) 2014;5:136–41.